Electric Power Systems Research 184 (2020) 106319

Contents lists available at ScienceDirect

Electric Power Systems Research

journal homepage: www.elsevier.com/locate/epsr

Electric distribution network reconfiguration optimized for PV distributed generation and energy storage

Raul Vitor Arantes Monteiro[a,*], Jakson Paulo Bonaldo[a], Raoni Florentino da Silva[b], Arturo Suman Bretas[c]

[a] Electrical Power Systems Operation and Smart Grid Research Lab., Federal University of Mato Grosso, Cuiabá, MT, Brazil
[b] Group for Innovation on Real Information System, Computing Engineering Department, Federal University of Mato Grosso, Campus Várzea Grande, Cuiabá, MT, Brazil
[c] Power Lab, University of Florida, Gainesville, FL, United States

ARTICLE INFO

Keywords:
Active power losses
System reconfiguration
Distribution grid
Energy storage system
Binary particle swarm optimization
Artificial Neural Networks

ABSTRACT

A new power grid PV-based generation technology presentes engineering challenges in regards to the control and operation of energy storage. Because the utility grid has bidirectional power-flow and further intelligent protection for intentional and unintentional islanding is required. Further, the high penetration of photovoltaics may increase active power losses, and reconfiguration studies must be conducted to analyze such losses and thus optimize system operation. Model based solutions become intractable considering the size of the search space. In this work a Binary Particle Swarm Optimization based solution is presented aiming distribution systems technical power losses reduction though system reconfiguration. Solution validation is carried on the IEEE 37 buses test feeder. A feasibility test is also addressed, and the results show that the BPSO and the use of energy storage systems are efficiently merged resulting in an electric distribution network reconfiguration optimized for PV distributed generation and energy storage, that can retrofit into existing power systems.

1. Introduction

Distribution networks have been design and operate passive elements, i.e., designed for unidirectional power flow from the source to the end-user. Therefore, the massive grid built in the last century is mostly not made to support the insertion of distributed generation (DG).

The connection of photovoltaic (PV) DGs to power systems does not respond to variations in the conditions of the electrical system in the same way as a conventional synchronous generator; the solar source has unique features, such as high-velocity response (low inertia) and high slew-rate for power ramps. Several studies, such as [1–3]. deal with the concerns associated with high penetration of distributed generation in distribution systems; such as consequences of voltage variations, frequency variations and the reduction of technical losses are highlighted. In regards to technical power losses minimization, a Particle Swarm Optimization (PSO) base solution is presented in this paper, showing efficiency and simplicity in its implementation [4].

Technical power losses minimization through distribution network reconfiguration is showing promising results. For example, in [5]. the authors introduced an ant colony search algorithm to solve the optimized network reconfiguration problem for power losses reduction. Such an ant colony algorithm has been compared to other two methods: a genetic algorithm optimization and a simulated annealing algorithm. The comparison showed that ant colony solution presented better results. To mitigate power quality disturbances, in [6]. a solution was presented to deal with harmonics, voltage sags and power losses minimization by network reconfiguration based on differential evolution algorithm. The reconfigured network showed the effectiveness of the proposed solution allowing the improvement of power quality indicators and decreasing of losses.

In [7]. an intelligent system for automatic reconfiguration of a distribution network based on branch exchange adaptation is used to solve real-time problems like losses reduction, load balance and the improvement of quality indicators. The authors tested the proposed methodology in a real grid, and the results showed an improvement in the network performance indicators. In [8]. the authors present a network reconfiguration strategy through the use of the binary group search algorithm. The optimization objective was the reduction of grid losses. According to the authors, the simulation of different test cases validated the proposed solution. Optimized distribution network reconfiguration with genetic algorithms was presented in [9]. for power quality and reliability improvement. The authors in [10]. proposed an evolutionary algorithm based on NSGA-II to tackle a multi-objective

* Corresponding author.
E-mail address: raulvitor@ufmt.br (R.V.A. Monteiro).

https://doi.org/10.1016/j.epsr.2020.106319
Received 5 August 2019; Received in revised form 17 January 2020; Accepted 6 March 2020
Available online 20 March 2020
0378-7796/

problem on a distributed network reconfiguration. The conclusions showed that the proposed method is capable of dealing with the uncertainties found in the analysis.

In [11]. an optimized distribution network reconfiguration for power loss minimization and voltage profile improvement is achieved through the cuckoo search algorithm. The simplicity of the algorithm showed that it could be an efficient method for distribution network reconfiguration problems. A robust reconfiguration for active losses minimization using the Most Probable Scenario (MPS) technique is presented by [12]. The authors use the receding horizon control concept, concluding that both techniques are suitable to handle the presented minimization problem. In [13]. the reconfiguration problem for power losses minimization is solved using a novel dynamic fuzzy c-means clustering based Artificial Neural Network (ANN). A very short processing time, simple structure, and high accuracy are claimed as the benefits of the proposed method. The power of the Binary Particle Swarm Optimization (BPSO) can be seen in [14]. The authors showed this algorithm is a powerful tool for losses reduction by performing distribution network reconfiguration while it can achieve global optimization.

Unlike the previous works, in this paper energy storage systems (EES) and artificial intelligence (AI) are used for optimized reconfiguration of electric energy distribution networks with photovoltaic penetration. For this purpose, a modified an IEEE 37-buses model test feeder is used as the application scenario. Such modifications were new paths introduced to the original test feeder so one can have alternative routes for the power flow.

The main contributions of the present work are:

- The design of a BPSO for the optimal topology for the distribution network regarding the minimization of technical power losses;
- The use of an ANN to estimate PV generation and perform of ESS for performance improvement of the reconfigured grid;
- The presented solution contributes to losses reduction by optimal reconfiguration of the distribution grid, not done before, as by the current state of art and literature.

The next sections are organized as follows: Section II presentes a summary of the BPSO. Section III presents the assumptions made in regards to feasibility features of the grid. Section IV brings the methodology used to achieve the results presented and discussed in section V.

2. Materials and methods

This section brings the tools and the methodology used to achieve the results presented in this work.

2.1. Binary PSO (BPSO)

The classic Particle Swarm Optimization (PSO) is designed for continuous optimization functions and not for discrete optimization functions. Hence, [15,16,28,29]. proposed a binary version for the PSO denominated as Binary Particle Swarm Optimization.

In electrical energy distribution systems, the reconfiguration of feeders is accomplished using the opening and closing of switching devices. The change in the position of these switches can reduce the losses on the lines or operate the system with greater security, as through the use of contingency methods. The structure that results from this switching should automatically obey the radial structure of a distribution system. For this configuration, the PSO can be used so that optimal topologies are found for the systems under study.

The primary objective of the distribution system reconfiguration is to minimize total technical losses on the lines during its normal operation. This problem can be formulated through (1):

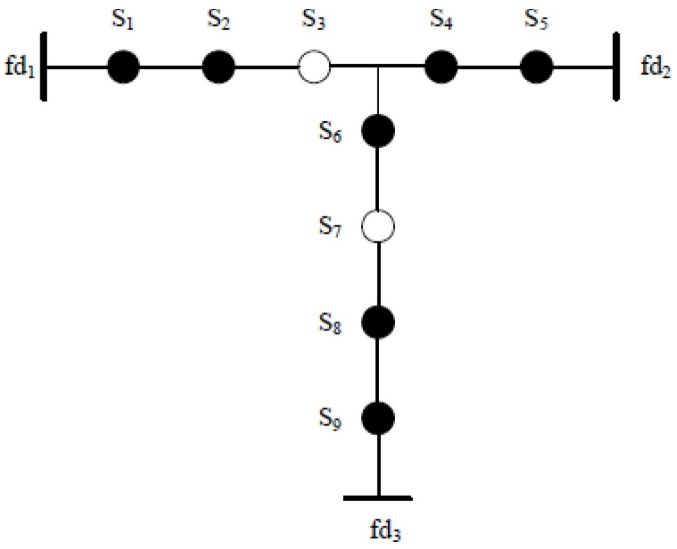

Fig. 1. [1,2] Initial configuration of the system used as an example (fd – feeder).

$$L_{losses} = \sum_{i=1}^{n} I_i^2 . R_i \tag{1}$$

where L_{losses} are the total technical losses of the distribution system, n is the total number of line stretches on the system, I_i is the electrical current value of the i *th* zone and R_i is the resistance of the i *th* line stretch.

To solve this problem, [16]. proposes a modified BPSO, which is the method used in this study. This method defines the Shift Operator (SO) and the Shift Operator Set (SOS). The reconfiguration problem of a distribution system can be treated as a combinatorial permutation optimization of '1′ and '0′, where a normally closed switch (NC) corresponds to '1′ and one that is normally open (NO) to '0′.

2.1.1. Shift operator (SO)

Let us suppose that a distribution system has a given quantity of NC and NO switches. The status of the switch combination NC + NO is $[S_1,S_2, \ldots, S_n]$ and will be called Sequence Switch States (SSS). As an example, a particle or individual can be represented by a sequence of zeros and ones. In this example, a particle is a binary vector with a set of NC + NO line stretches. For a system that contains in its configuration 9 switches, as shown in Fig. 1, the SSS then becomes:

$$sss = x\frac{k}{i} = \left[\frac{s_1, s_2, s_3, s_4, s_5, s_6, s_7 s_8 s_9}{[1{\cdot}1{\cdot}0{\cdot}1{\cdot}1{\cdot}1{\cdot}0{\cdot}1{\cdot}1]}\right] \tag{2}$$

The SO is defined as a vector of three dimensions, which stores the following information:

1 Which solution bit will be shifted;
2 In which direction this bit will be shifted (right (R) or left (L));
3 How many positions the bit will be shifted according to the attributed direction.

The new SSS permutation is defined by SSS' = SSS ⟨+⟩ SO. The symbol ⟨+⟩ indicates that the shift operator was applied to the SSS vector.

For example, Fig. 2 illustrates the application of the SO on the SSS, resulting in SSS'. The new set of zeros and ones for the given particle or

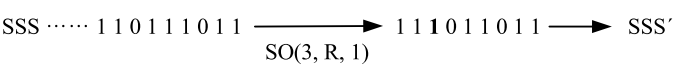

Fig. 2. Application of the shift operator SO.

individual after the shift operator has been applied. As one can see, the shift operator moved the third bit (0), one position to the right direction (3, *R*, 1).

2.1.2. Shift operator set (SOS)

The shift operator (SO) can contain more than one operation, i.e., a set of operations can be performed over the same step. An example would be to imagine two operators SO_1 and SO_2. Through the fusion between the two operators, it is obtained the resulting shift operator SOS, such that $SOS = \{SO_1, \cdot SO_2\} = SSS_1 \cdot \ominus \cdot SSS_2$ Where SSS_1 and SSS_2 are two particles or solutions (different switching sequences NO and NC). The SOS is in fact found by comparing,the switch positions one by one. The operator $\ominus$ is used to indicate the generation of the shift operators SSS_1 and SSS_2.

2.1.3. Modified BPSO

With the definition of the necessary operators given by the modified algorithm, the BPSO can be defined for solving reconfiguration problems of electric energy distribution system topologies by applying (3) into (4).

$$x_i^{k+1} = x_i^k + V_i^{k+1} \tag{3}$$

where,

x_i^{k+1} is the position of one particle at instant time $k + 1$;

x_i is the position at instant time k;

V_i^{k+1} is the new and adjusted velocity the will be applied to the particle.

$$V_i^{k+1} = (w \otimes V_i) \oplus (rand() \langle \times \rangle (pbest \ominus x_i)) \oplus (rand() \langle \times \rangle (gbest \ominus x_i)) \tag{4}$$

where,

w is the inertia operator;

V_i is the velocity at time k;

pbest is the best personal position of the particle;

gbest is the best global position among all particles;

x_i is the actual position of particle *i*.

The function of the operator w is maintained in this process for adjustments to the search areas. The approach of the BPSO model adopted consists of increasing or decreasing the step to be taken by the shift operator at each iteration. Thereby, $\otimes$ it applies the value from w calculated to the size of the operator that consists of the shift step.

The composition of the coefficient *rand()* with the symbol $\times$ executes an operation, for which the action is to randomly choose a shift operator from among the operators grouped in $(pbest \ominus x_{id})$ and $(gbest \ominus x_{id})$.

In the previous example Fig. 2), according to the resulting SO, bit 3 was shifted to the right, represented by the letter *R*, position 1. In this operation, for the system radiality to be maintained, only 2 switches could remain open. Thus, the switch that corresponds to 3 (S_3) went from the NO (0) state to the NC (1) state. Therefore, the new configuration of the system is presented in Fig. 3.

The procedure for the implementation of the PSO algorithm follows the steps as laid out in [16].

1 Choose the size of the population (different binary vectors that contain combinations of NO and NC switches), as well as the maximum number of desired iterations;
2 Initiate the SSS and the shift operators SO randomly for applying to the particles;
3 For each particle evaluate the desired optimization fitness function;
4 Compare the evaluation from step 2 with the *pbest* from each particle. If the current value is better than the previous value, then update the current *pbest* as the new *pbest*, including the SSS and the value of the fitness for *pbest*;
5 Compare the evaluation of each *pbest* with the previous best evaluation value of the population. If the actual value is better than the previous *gbest*, then update the value of *gbest*, including the SSS and the value of the *gbest* fitness;
6 Update the shift operator SO and generate a new state of operation for the switches (SSS) and the fitness value for the *gbest*;
7 Repeat the process from step 3 until a stop criterion is satisfied; this generally means a maximum number of iterations, in a manner that this number is adequate for guaranteeing a good quality fitness function.

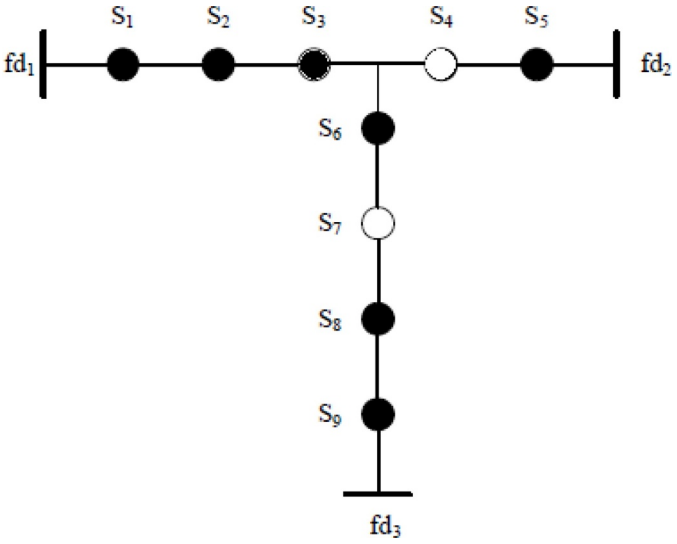

Fig. 3. Final configuration of the system after the applied SO.

Fig. 4. shows the flow chart for the algorithm used.

2.2. A technique for verifying isolated busses in the distribution system (DS)

Several different system topologies can be represented using diagrams composed of a set of points and lines that link together. For example, the points can be the corners of a city and the lines the streets; also the points can be cities and the lines flight paths taken by planes; or even, the points can be buses on an electrical system and the lines, its transmission or distribution lines. The mathematical abstraction of situations of this type gives rise to the graph concept.

The most practical means for representing the connectivity between busses in the DS is using chain graphs. An energy distribution system, in light of its radiality, can be represented by a graph forest. In this section, an introduction to the graph theory is presented, along with a simple method to represent a radial system.

By taking as an example the graph in Fig. 5. and considering each vertex as a bus and each edge as a line of a distribution system, the first step is to obtain the charting of the lines relating its bus terminals and their origins. To conclude such, numbers substituted the nomenclature of the vertexes and edges to facilitate the understanding of the method used, which resulted in Fig. 5.

Table 1 is used to determine the connectivity of each bus.

As of this point, the concept of the adjacency matrix and Laplacian matrix is used [17]. and we will call the graph represented in Fig. 5. as G.

Given graph G = (V,E) with n vertexes, the adjacency matrix of matrix G is the matrix of order n given by A(G) = $[a_{ij}]$, here $a_{ij} = 1$ if $v_i v_j \in$ E, being E the energy of the graph, and $a_{ij} = 0$ in the remaining inputs.

The Laplacian matrix of G is the matrix of order n given by L (G) = $[l_{ij}]$, where $l_{ij} = -1$ if $v_i v_j \in$ E, $l_{ij} = d(v_i)$ and $l_{ij} = 0$ in the remaining inputs. The Laplacian matrix and the adjacency matrix are related in the following manner (5):

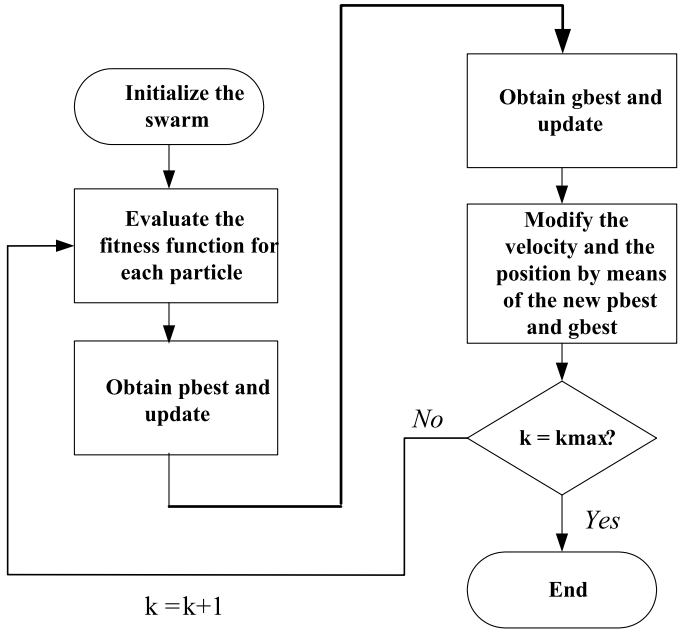

Fig. 4. Flow chart of the BPSO.

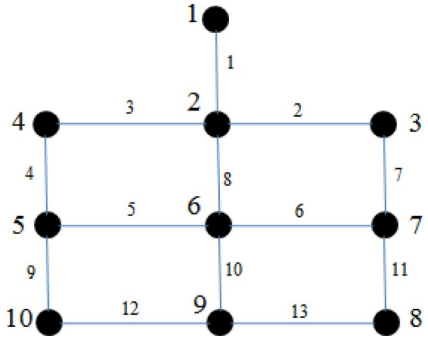

Fig. 5. Representation of an electric matrix system.

Table 1
Connectivity of the buses of the system represented in Fig. 5.

Line	Initial bus	End bus
1	1	2
2	2	3
3	2	4
4	4	5
5	5	6
6	6	7
7	3	7
8	2	6
9	5	10
10	6	9
11	7	8
12	10	9
13	9	8

$$L = D - A \tag{5}$$

Where D is the diagonal matrix with the degrees of the vertexes. In a manner to exemplify this theory, the following example is given.

Matrix a is formed in a way that its lines and columns correspond to the number of buses on the system, thus obtaining a square matrix. In this specific case, one has a matrix of 10×10. The value -1 is attributed to indicate the connectivity between buses. The buses that do not possess connectivity between one another receive the value 0. For example, to the element $a_{2,\ 3}$ of matrix a it is attributed the value -1, indicating the connectivity between the buses 2 and 3. However, in $a_{2,\ 10}$, the value 0 is attributed, since bus 2 does not possess connectivity with bus 10. This process is performed over all buses, and finally, the values attributed to each column of matrix a are summed together and stored on the main diagonal that corresponds to each bus. To provide a better understanding of this concept, another example is given.

If we consider that, no line is open, matrix a would have the composition shown in Fig. 6.

It is verified that the sums for the values stored on the columns corresponding to each bus were added together and attributed to the main diagonal line of the matrix. Now, consider that line 2, and line 6 of the system represented in Fig. 6. are removed from the configuration. Matrix a will change its composition, as shown in Fig. 7.

Using Fig. 7, one can see on the highlighted elements that the values attributed to the main diagonals, which correspond to buses that the removed lines were connected to, in fact, received a reduction in their values. This way, the summation results on the diagonals corresponding to buses 2, 3, 6, and 7 (Fig. 5), is lower than those in Fig. 6.

The feasibility thus consists of detecting which configurations from matrix a are permitted and which are not, so that the system is solvable or feasible. Therefore, it can be checked by the elements of the main diagonal that present the value 0. This would mean that the bus which corresponds to that column is isolated. Hence, the system would isolate

$$a = \begin{vmatrix} -1 & -1 & 0 & 0 & 0 & 0 & 0 & 0 & 0 & 0 \\ -1 & -4 & -1 & -1 & 0 & -1 & 0 & 0 & 0 & 0 \\ 0 & -1 & -2 & 0 & 0 & 0 & -1 & 0 & 0 & 0 \\ 0 & -1 & 0 & -2 & -1 & 0 & 0 & 0 & 0 & 0 \\ 0 & 0 & 0 & -1 & -3 & -1 & 0 & 0 & 0 & -1 \\ 0 & -1 & -1 & 0 & -1 & -4 & -1 & 0 & -1 & 0 \\ 0 & 0 & 0 & 0 & 0 & -1 & -3 & -1 & 0 & 0 \\ 0 & 0 & 0 & 0 & 0 & 0 & -1 & -2 & -1 & 0 \\ 0 & 0 & 0 & 0 & 0 & -1 & 0 & -1 & -3 & -1 \\ 0 & 0 & 0 & 0 & -1 & 0 & 0 & 0 & -1 & -2 \end{vmatrix}$$

Fig. 6. Matrix a for the case where all lines are active.

$$a = \begin{vmatrix} -1 & -3 & 0 & -1 & 0 & -1 & 0 & 0 & 0 & 0 \\ 0 & 0 & -1 & 0 & 0 & 0 & -1 & 0 & 0 & 0 \\ 0 & -1 & 0 & -2 & -1 & 0 & 0 & 0 & 0 & 0 \\ 0 & 0 & 0 & -1 & -3 & -1 & 0 & 0 & 0 & -1 \\ 0 & -1 & -1 & 0 & -1 & -3 & 0 & 0 & -1 & 0 \\ 0 & 0 & 0 & 0 & 0 & 0 & -2 & -1 & 0 & 0 \\ 0 & 0 & 0 & 0 & 0 & 0 & -1 & -2 & -1 & 0 \\ 0 & 0 & 0 & 0 & 0 & -1 & 0 & -1 & -3 & -1 \\ 0 & 0 & 0 & 0 & -1 & 0 & 0 & 0 & -1 & -2 \end{vmatrix}$$

Fig. 7. Matrix *a* for the case of lines 2 and 6 as inactive or open.

one bus, and as such, a solution with this type of configuration would not be feasible. The higher the complexity of the system, the higher will be the number of analyses and cases for observation, thus arriving at the possibility of iterative methods.

2.3. Methodology

To validate the performance of the BPSO optimization algorithm, three case studies were performed, and the modified IEEE 37 bus test feeder was considered, as shown in Fig. 8. The modification is the addition of distributed generators on the buses 710, 711 and 741. The distributed generators were placed in these sites because they are further from the principal source (bus 799), which allows them to have a greater effect in the whole system. It should be emphasized that the system losses without the topology change and addition of energy storage system were of 0.03921 p.u.

For this study, static analysis was made, i.e., variable demand (multi-intervals optimization) was not considered. Therefore, the power flow of loads and power injections are related to the period when the maximum PV generation occurs. An ANN estimates the PV generation, and its data were used in cases 2 and 3. This information can be found in the next section (2.3.1). Moreover, the power flow, the BPSO, and the feasibility test algorithms were developed in MatLab script.

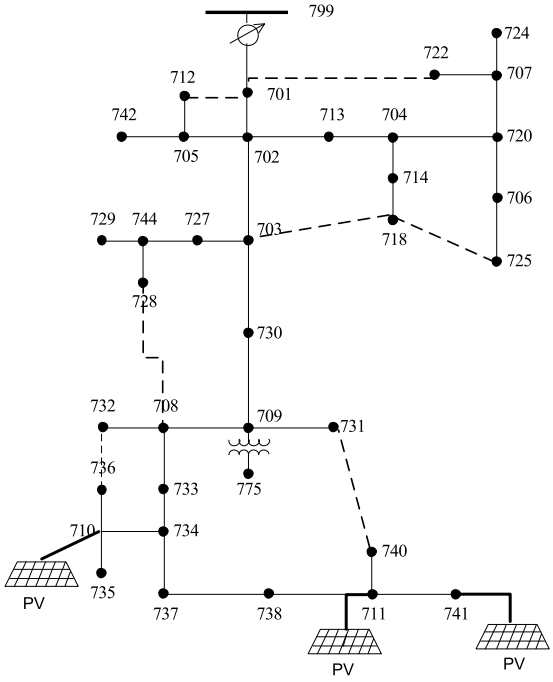

Fig. 8. Modified IEEE 37 bus system.

As the system is purely radial without distributed resources (distributed generators), the addition of alternative routes becomes necessary, thus creating a looped system. Moreover, the extra cost through the addition of new sections should not be taken into consideration. Therefore, one should treat the system as though it already exists in the manner proposed and illustrated in Fig. 8.

Notice from Fig. 8. that the following sections were activated:

- 712–701;
- 701–722;
- 703–718;
- 718–725;
- 728–708;
- 732–736;
- 730–741.

All the added sections were attributed with the same line parameters as those from section 701-702, as a greater part of the power flow is originally found in this section. However, the condition that is not enough for a topology to be radial is found in (6) [18].

$$\text{Lines} = \text{buses} - 1 \tag{6}$$

With,

Lines – the number of lines from the system;

Buses – the number of buses from the system.

The number of switches that can be open for the reconfiguration can be determined by (7):

$$\text{Switches} = \text{Lines}_{\text{m}} - \text{Lines}_{\text{r}} \tag{7}$$

Where,

$Lines_m$ – is the number of lines from the looped system;

$Lines_r$ – is the number of lines from the radial system.

Therefore, for the case under analysis, a total of 5 switches should be open for reconfiguration, since the system possesses 42 lines after the modifications.

The search space for the problem can be obtained through combinatory analysis, where the number of combinations for *NB* elements taken *N* to *N* is defined as (8) [19].

$$C_{NB}^{N} = \frac{NB!}{N!(NB-N)!} \tag{8}$$

According to (8), the search space results in 850,668 possibilities, thus justifying the use of an optimization algorithm for solving this problem.

The objective optimization function is given by (9):

$$Min \sum (R.\, I^2)^{\rho} \tag{9}$$

Where,

$(R.I^2)^{\rho}$ – Active losses in phases *a, b* and *c*;

ρ – *Phases a, b and c.*

The set of restrictions used for this problem are related to the power flow calculation by the Newton-Raphson algorithm. As discussed in [3]. these restrictions may be given by (10), (11), and (12).

Subject to:

$$V_{min}^{\rho} \le V_{i,k}^{\rho} \le V_{max}^{\rho} \tag{10}$$

$$PI_{i}^{\rho} - PD_{i}^{\rho} - \sum P_{i,k}^{\rho} = 0 \tag{11}$$

$$QI_{i}^{\rho} - QD_{i}^{\rho} - \sum Q_{i,k}^{\rho} = 0 \tag{12}$$

where,

V_{min}^{ρ} is the minimum voltage magnitude of the three phases;

V_{max}^{ρ} is the maximum voltage magnitude of the three phases;

PI_{i}^{ρ} is the active power injected onto node *i* for the three phases;

PD_{i}^{ρ} is the active power drained onto node *i* for the three phases;

QI_{i}^{ρ} is the reactive power injected onto node *i* for the three phases;

Table 2
ANN structure.

Architecture	Technique	No. of layers	Hidden neuron	Tapped delay-time	Activation function / Hidden layer	Activation function / output layer
NARX	Bayesian Regularization (BR)	2	10	2	Tangent-Sigmoid	Linear

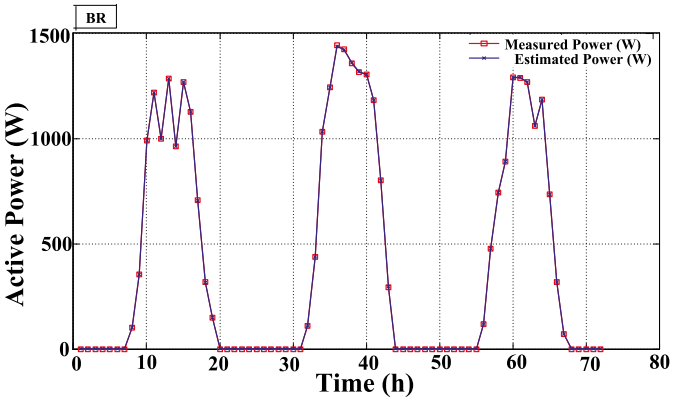

Fig. 9. Measured power (W) and estimated power (W) for 72 h.

QD_i^{ρ} is the reactive power drained onto node *i* for the three phases;
$P_{i,k}^{\rho}$ is the active power flow that goes from node *i* to node *k* from the three phases;
$Q_{i,k}^{\rho}$ is the reactive power flow that goes from node *i* to node *k* for the three phases.

2.3.1. Prediction of photovoltaic generation

An ANN estimated the photovoltaic generation according to the procedure described in [20]. The ANN structure is given in Table 2. The prediction is performed based on meteorological data collected from the Brazilian National Institute for Space Research (INPE) of Uberlândia city (MG) in Brazil. Fig. 9. shows a comparison between the measured data and the estimated data. Therefore, the resulting PV peak generation determined by the ANN was 1269 kW.

As can be seen in Fig. 9, the forecast horizon is 72 h. Initially, the ANN was trained to estimate PV generation just depending on how much of irradiation, environment and solar panels temperature data information the user has. As an example, a 72 h forecast has been computed and shown in the aforementioned figure.

A real system to collect the ANN training data and then scaled the PV system to simulate it on the 37 bus test feeder was used. The power inverter used in the real system is the PHB3000-NS which rated power is 3000 W. The minimum MPPT (Maximum Power Point Tracking) voltage is 80 V. Due to its low DC voltage this inverter is able to operate in low irradiance conditions generating low output power in the AC side.

2.3.2. Electrical energy storage (ESS) scaling

The methods used to determine the size of the ESS have been shown in [21]. From the analyses developed in the previous section, the system peak demand was defined as 2457 kW and the PV peak generation on 1269 kW. Similarly to [22]. the EES was limied to 10% of the difference between the nominal values of photovoltaic generation and maximum demand. Otherwise, the sized values would be difficult to achieve.

For better comprehension, Table 3 shows a summary from the system considered.

The system's demand and photovoltaic (estimated) profiles are shown in Fig. 10.

Table 3
Power system parameters.

Quantity	kW	kWh
System Peak Demand	2457	–
PV Peak Generation	1269	–
Energy Storage Capacity	110	54.000

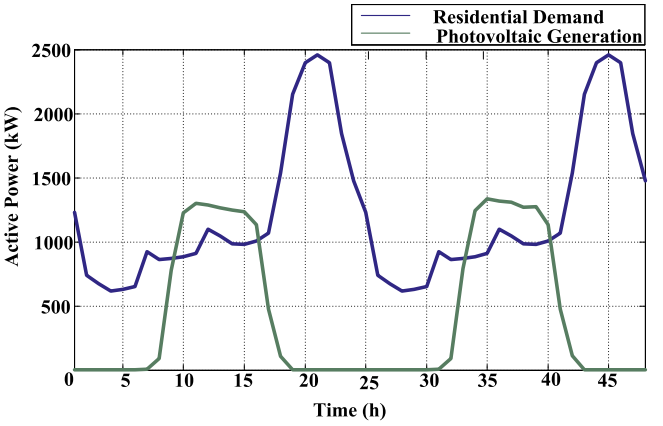

Fig. 10. Power demand versus photovoltaic generation.

3. Results and discussion

To demonstrate the effectiveness of the BPSO algorithm, the optimization process was done for three different situations:

- Case I: BPSO performance was evaluated with the nominal load, without considering DG;
- Case II: the second case takes into account the maximum PV generation on buses 710, 711, 741; and the nominal demand load level;
- Case III: the third case considers the situation for the highest PV generation (buses 710, 711 and 741) and the real system demand at the considered day time (this scenario is close to a real case);

Firstly, except for the case III, all the cases were simulated considering ESS injection at bus 738 and, then no considering ESS injection in all cases. As for the batteries modelling, in the power flow calculation they were inserted as load with unitary power factor when charging, and as a generator, i.e. injecting active power, with unitary power factor when discharging.

As the information concerning to the optimal value for this optimization was not available, the option was made for testing the number of particles until achieving 100 particles. Each of the particles quantities was tested with 100 iterations. The first case was used for this task. Fig. 11. presents the best results reached for the particles quantities. The computer used for these simulations was an iMac with a processor of 4 GHz Intel Core i78 and 32 GB of RAM.

By analyzing Fig. 11, one finds that the algorithm converges. The tests with 60 particles for 100 iterations, the algorithm reached its best result overall remaining quantities, except for the optimization with 80 particles, which obtained the same result. However, as intended to

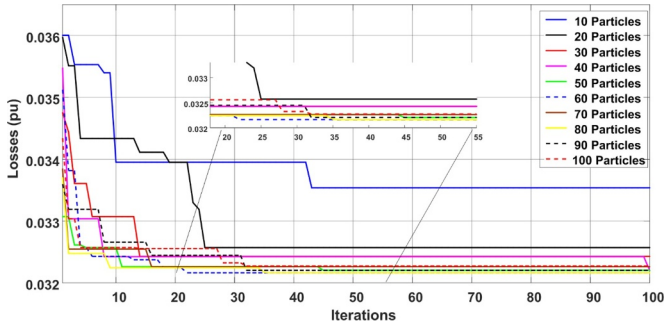

Fig. 11. BPSO convergence.

Table 4
Several particles, open stretches, and losses in pu – S_{base} = 1 MVA.

Number of particles	Topology	Losses (pu)	Average
10	5, 10, 19, 21, 28	0.03354	0.032775
20	10, 11, 12, 21, 42	0.03257	0.03245
30	5, 10, 11, 12, 20	0.03243	0.032515
40	5, 10, 11, 28, 42	0.0322	0.032235
50	5, 10, 11, 28, 42	0.0322	0.03223
60	5, 10, 12, 29, 42	0.03209	0.0322
70	5, 10, 15, 25, 28	0.03226	0.032345
80	5, 10, 15, 28, 37	0.03216	0.032205
90	5, 10, 11, 28, 42	0.0322	0.032235
100	10, 11, 25, 28, 37	0.03227	0.03222

Table 5
Stretches and assigned numbering.

Stretches	Assigned Numbering	Stretches	Assigned Numbering		
799	701	1	709	731	22
701	702	2	709	708	23
701	712	3	710	735	24
701	722	4	710	736	25
702	705	5	711	741	26
702	713	6	711	740	27
702	703	7	713	704	28
703	727	8	714	718	29
703	730	9	720	707	30
703	718	10	720	706	31
704	714	11	727	744	32
704	720	12	730	709	33
705	742	13	733	734	34
705	712	14	734	737	35
706	725	15	734	710	36
718	725	16	737	738	37
707	724	17	738	711	38
707	722	18	744	728	39
708	733	19	744	729	40
708	732	20	740	731	41
728	708	21	732	736	42

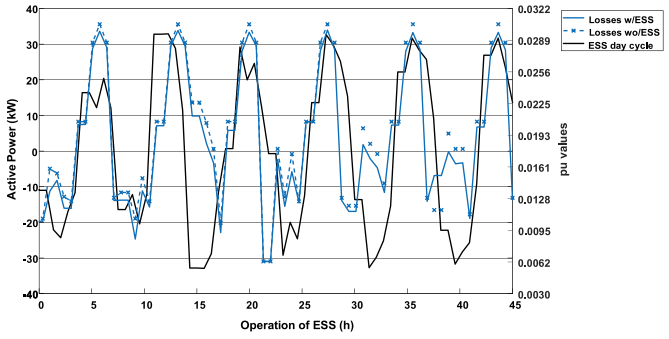

Fig. 12. EES day cycle, losses profile with and without EES.

optimize, it should be taken into consideration that the more particles one uses, greater will be the computational time spent. Thus, it is recommended that for this case, 60 particles are used for 100 iterations. In this way, these quantities were used for the other three cases as well.

By Table 4 shown below, one notes that the algorithm converges at the value of 0.032 p.u, since the average of the 10 results obtained from the simulations for each quantity of particles presents this convergence.

Table 5 presents the enumeration given to the stretches of line, while Table 4 shows for each quantity of particles, the sequence of open sections that presented the best results over the optimization process. On Table 5, the sections in red are the additional sections.

The second case is a situation in which the system is with its highest demand load level, highest PV generation, and ESS, according to Table 3.

For the third case, a simulation closest to a real case was performed, and here is where the ANN prediction is justified. For this case, according to Fig. 10, one can see that the highest DG penetration occurs at hour 14:00 (2:00 pm), corresponding to a 42.49% lower than the nominal load level observed in [23]. However, for comparison purposes, a 50% lower load level was considered. Once the DG generation is higher than the load demand, in this case, study, the use of ESS was not necessary.

Four tests were performed to evaluate the best ESS position on the system, taking into account concentrated and distributed locations. For the concentrated topology, in the first test, the EES was placed on bus 730. In the second test, the ESS is placed on bus 738. Regarding the distributed topology, the third test is carried out with the placement of EES on buses 701, 730, 738 and, in the fourth test, buses 724, 729 and 738 are chosen to receive the ESS. According to [23] the best topology was found in the second case, or be it, the lower losses experienced by the test feeder had the EES housed on bus 738. Table 7 shows the comparison between the losses with and without EES for the sequence of open stretches encountered by the BPSO optimization with 60 particles and 100 iterations.

Fig. 12. shows the ESS operating during 5 days. Highlight that only the time in which ESS is charging or discharging is considered, i.e., the hours in which the ESS is not used in the charge-discharge mode were removed. Thus, notice that, in this interval, 5 cycles of charging/discharging are performed showing the losses with and without ESS. Each cycle represents one complete charge-discharge cycle per day. Following the process outlined in Fig. 2, a positive value ("y" left axis) means that the ESS is discharging power, and a negative value means that the ESS is in charging mode. For example, between 6 and 10 h, shows the ESS operating in the charging mode, i.e., when the grid demand is growing and gets to its peak, and the PV generation is decreasing. The values on the right "y" axis show the losses performance with and without ESS.

Table 6 summarizes the results of the three case studies.

The results in Table 6 show that a considered loss reduction was achieved by the BPSO algorithm. For case 1, compared with the base case, an 18.15% losses reduction has been achieved, and when considering ESS, the reduction increased to 26.57%. Case study 2 resulted in a high reduction of 76.43% and 77.50% when considering ESS. Finally, case study 3 got a 47.64% of losses reduction.

Once one has a 72 h PV generation estimation, the proposed algorithm could be used between these hours. However, for a smaller error result, a 24 h usage is recommended, once meteorological conditions are too volatile.

It is not an easy task to compare these results with other results in the literature. However, one can do this with systems with more than 30 buses. The results of the BPSO algorithm presented in this paper are compared according to the same case studies investigated by the referenced papers in the last column. As one can see in Table 7, the tested approach had a response better than other approaches. The camparison made takes into account two multi-intervals optimizations, refs. [24]. and [25].

Table 6
The performance of the BPSO for all the case studies – Sbase = 1 MVA.

Base	Parameters	Case study 1	Case study 2	Case study 3
No Reconfiguration	Losses (p.u)	0.03921	0.03921	0.0085
With Reconfiguration	Losses (p.u)	0.03209	0.00924	0.00445
	Switches	5, 10, 12, 29, 42	12, 28, 31, 39, 42	3, 4, 11, 12, 23
	Losses with ESS (p.u)	0.02879	0.00882	–
	Switches	5, 6, 10, 20, 29	11, 12, 15, 39, 42	

Table 7
Literature comparison.

Algorithm	CLONALG	Copt-aiNet	Copt-aiNet / Opt-aiNet	IEPSO	BPSO without energy storage	BPSO with energy Storage
Buses	87	87	84	33	37	37
Compared case	1	1	1	1 3	1 3	1
Reduction	10.05	10.05	11.66	23.26 17.98	18.15 47.64	26.57
Reference	[24]	[25]	[26]	[27]	Here	Here

4. Conclusion

The BPSO algorithm demonstrated high efficiency for the optimization of an electric energy distribution system, approaching at minimizing losses. There is a big data analytics scenario, with 850,668 topological possibilities, that makes the task of finding a good topology difficult through iterative brute-force methods, and only AI can handle such a problem.

The convergence of the BPSO for this case returned a value of 0.032 p.u., following the average retrieved from the simulations performed for the number of particles and the number of iterations presented. The best topology encountered needed 60 particles and 100 iterations to be discovered. Three case studies have been simulated to show the advantage of the BPSO algorithm.

Finally, it was concluded that for optimization processes, the use of the BPSO in the reconfiguration of electric energy systems had shown itself to be a viable and functional tool.

Credit author statement

Author Contributions: Raul Vitor Arantes Monteiro and Jakson Paulo Bonaldo, developed the idea, designed, and performed the simulations. Raoni Florentino Teixeira and Arturo Suman Bretas, contributed to the overall concept development, methodology, data analysis, writing of the paper and of the revised version, editing the manuscript. All authors have read and approved the final manuscript.

Declaration of Competing Interest

The authors declare that they have no known competing financial interests or personal relationships that could have appeared to influence the work reported in this paper.

References

[1] M.Z. Degefa, M. Lehtonen, R.J. Millar, A. Alahäivälä, E. Saarijärvi, Optimal voltage control strategies for day-ahead active distribution network operation, Elect. Power Sys. Res. 127 (2015) 41–52, https://doi.org/10.1016/j.epsr.2015.05.018.

[2] Golmohamadi, H.; Keypour, R. Application of robust optimization approach to determine optimal retail electricity price in presence of intermittent and conventional distributed generation considering demand response. J. Control Autom. Electr. Syst., vol 28, pp. 661–678. 10.1007/s40313-017-0328-9.

[3] Ismail, M.M. Protection of Three-Phase VSI grid connected PV system during transient conditions using fuzzy logic. J. Control Autom. Electr. Syst., vol 24, pp. 189–200. 10.1007/s40313-015-0224-0.

[4] T. Soares, F. Pereira, H. Morais, Z. Vale, Cost allocation model for distribution networks considering high penetration of distributed energy resources, Elect. Power Sys. Res. 124 (2015) 120–132, https://doi.org/10.1016/j.epsr.2015.03.008.

[5] C. Su, C. Chang, J. Chiou, Distribution network reconfiguration for loss reduction by ant colony search algorithm, Elect. Power Sys. Res. 75 (2005) 190–199, https://doi.org/10.1016/j.epsr.2005.03.002.

[6] S. Jazebi, B. Vahidi, Reconfiguration of distribution networks to mitigate utilities power quality disturbances, Elect. Power Sys. Res. 91 (2012) 9–17, https://doi.org/10.1016/j.epsr.2012.04.008.

[7] L.L. Pfitscher, D.P. Bernardon, L.N. Canha, V.F. Montagner, V.J. Garcia, A.R. Abaide, Intelligent system for automatic reconfiguration of distribution network in real time, Elect. Power Sys. Res. 97 (2013) 84–92, https://doi.org/10.1016/j.epsr.2012.12.007.

[8] S. Teimourzadeh, K. Zare, Application of binary group search optimization to distribution network reconfiguration, Int. J. Electr. Power Energy Syst. 62 (2014) 461–468, https://doi.org/10.1016/j.ijepes.2014.04.064.

[9] N. Gupta, A. Swarnkar, K.R. Niazi, Distribution network reconfiguration for power quality and reliability improvement using Genetic Algorithms, Int. J. Electr. Power Energy Syst. 54 (2014) 664–671, https://doi.org/10.1016/j.ijepes.2013.08.016.

[10] C. Henrique, N. De Resende, M. Henrique, S. Mendes, Robust feeder reconfiguration in radial distribution networks, Int. J. Electr. Power Energy Syst. 54 (2014) 619–630, https://doi.org/10.1016/j.ijepes.2013.08.015.

[11] T. Thanh, A. Viet, Distribution network reconfiguration for power loss minimization and voltage profile improvement using cuckoo search algorithm, Int. J. Electr. Power Energy Syst. 68 (2015) 233–242, https://doi.org/10.1016/j.ijepes.2014.12.075.

[12] P. Chittur, J. Tant, J. Radhakrishna, Novel methodology for optimal reconfiguration of distribution networks with distributed energy resources, Elect. Power Sys. Res. 127 (2015) 165–176, https://doi.org/10.1016/j.epsr.2015.05.005.

[13] H. Fathabadi, Power distribution network reconfiguration for power loss minimization using novel dynamic fuzzy c-means (dFCM) clustering based ANN approach, Int. J. Electr. Power Energy Syst. 78 (2016) 96–107, https://doi.org/10.1016/j.ijepes.2015.11.077.

[14] R. Pegado, Z. Ñaupari, Y. Molina, C. Castillo, Radial distribution network reconfiguration for power losses reduction based on improved selective BPSO, Elect. Power Sys. Res. 169 (2019) 206–213, https://doi.org/10.1016/j.epsr.2018.12.030.

[15] C.R. Eberhart, Y. shi, Guest editorial special issue on particle swarm optimization, IEEE Trans. Evol. Comp. 8 (3) (2004) 201–203, https://doi.org/10.1109/TEVC.2004.830335.

[16] W. Wu, M. Tsai, F. Hsu, A new binary coding particle swarm optimization for feeder reconfiguration, Intell. Syst. Appl. Pow. Syst. ISAP (2007) 1–6.

[17] J. Brooks, P Barooah, Consumer-aware load control to provide contingency reserves using frequency measurements and inter-load communication, Am. Control Conf. (ACC) (Jul. 2016) 5008–5013, https://doi.org/10.1109/ACC.2016.7526147.

[18] S. Civanlar, J.J. Grainger, S.S.H. Lee, Distribution feeder reconfiguration for loss reduction, IEEE Trans. Power Deli. 3 (1988) 1217–1223, https://doi.org/10.1109/61.193906 n. 3.

[19] J. Ubirajara, N. Nunes, A.S. Nunes, Voltage regulators allocation in power distribution networks : a Tabu search approach, 19 Th Int. Conf. Intell. Syst. Appl. Pow. Syst. (Sep. 2017), https://doi.org/10.1109/ISAP.2017.8071379.

[20] R.V.A. Monteiro, G.C. Guimarães, F.A.M. Moura, M.R.M.C. Albertini, M.K. Albertini, Estimating photovoltaic power generation: performance analysis of artificial neural networks, Support Vector Machine and Kalman filter, Elect. Power Sys. Res. 143 (2016) 643–656, https://doi.org/10.1016/j.epsr.2016.10.050.

[21] R.V.A. Monteiro, G.C. Guimarães, F.A.M. Moura, M.R.M.C. Albertini, F.B. Silva, Long-term sizing of lead–acid batteries in order to reduce technical losses on distribution networks: a distributed generation approach, Elect. Power Sys. Res. 144 (Dec. 2016) 163–174, https://doi.org/10.1016/j.epsr.2016.12.004.

[22] R. Dufo-lópez, J.M. Lujano-rojas, J.L. Bernal-Agustín, Comparison of different lead – acid battery lifetime prediction models for use in simulation of stand-alone photovoltaic systems, Appl. Energy 115 (Nov. 2014) 242–253, https://doi.org/10.1016/j.apenergy.2013.11.021.

[23] R.V.A. Monteiro, G.C. Guimarães, F.B. Silva, R.F.S. Teixeira, B.C. Carvalho, A.P. Finazzi, A.B Vasconcellos, A medium-term analysis of the reduction in technical losses on distribution systems with variable demand using artificial neural networks: an Electrical Energy Storage approach, Energy 164 (Sep. 2018)

1216–1228, https://doi.org/10.1016/j.energy.2018.09.021.
[24] Souza, S.S.F.; Romero, R.; Pereira, J.; Saraiva, J.T. Reconfiguration of radial distribution systems with variable demands using the clonal selection algorithm and the specialized genetic algorithm of Chu-Beasley. J. Control Autom. Electr. Syst., vol 27, pp. 689–701. 10.1007/s40313-016-0268-9.
[25] S. Souza, F. S., R. Romero, J. Pereira, J.T. Saraiva, Artificial immune algorithm applied to distribution system reconfiguration with variable demand, Intern. J. Elec. Pow. Syst. Res. 82 (2016) 561–568, https://doi.org/10.1016/j.ijepes.2016.04.038.
[26] S.S.F. Souza, R. Romero, J. Pereira, J.T. Saraiva, Artificial immune networks Copt-aiNet and Opt-aiNet applied to the reconfiguration of radial electrical systems, Elec. Pow. Syst. Res. 119 (2015) 304–312, https://doi.org/10.1016/j.epsr.2014.10.012.
[27] N.F. Napis, A. Fazliana, A. Kadir, T. Khatib, E.E. Hassan, An improved method for reconfiguring and optimizing electrical active distribution network using evolutionary particle swarm optimization, Appl. Sci. 8 (2018) 804–822, https://doi.org/10.3390/app8050804.
[28] G. Pampara, N. Franken, A.P. Engelbrecht, Combining particle swarm optimisation with angle modulation to solve binary problems, 2005 IEEE Congr. Evolut. Comput. Edinburgh, Scotland 1 (2005) 89–96, https://doi.org/10.1109/CEC.2005.1554671.
[29] M. Baioletti, A. Milani, V. Santucci, Algebraic particle swarm optimization for the permutations search space, 2017 IEEE Congr. Evolut. Comput. (CEC), San Sebastian (2017) 1587–1594.